MedChemComm

Accepted Manuscript

This article can be cited before page numbers have been issued, to do this please use: B. Mathew, S. Cheol Baek, D. Grace Thomas Parambi, J. Pil Lee, M. Joy, A. Rilda, R. Ranadev, P. nithymol, V. Vijayan, S. t. inasu, G. E. Mathew, K. K. Lohidhakshan, G. Kumar Krishnan and H. kim, *Med. Chem. Commun.*, 2018, DOI: 10.1039/C8MD00399H.

ROYAL SOCIETY OF CHEMISTRY

rsc.li/medchemcomm

View Article Online
DOI: 10.1039/C8MD00399H

View Article Online
DOI: 10.1039/C8MD00399H

Selected aryl thiosemicarbazones as new class of multi-targeted monoamine oxidase inhibitors

Bijo Mathew[1*#], Seung Cheol Baek[2#], Della Grace Thomas Parambi[3], Jae Pil Lee[2], Monu Joy[4], P.R. Annie Rilda[1], Rugma V. Randev[1], P. Nithymol[1], Vijitha Vijayan,[1] Sini. T. Inasu[1], Githa Elizabeth Mathew[5], Krishnakumar K. Lohidakshan[6], Girish Kumar Krishnan[7], Hoon Kim[2*]

[1] Division of Drug Design and Medicinal Chemistry Research Lab, Department of Pharmaceutical Chemistry, Ahalia School of Pharmacy, Palakkad-678557, Kerala, India

[2] Department of Pharmacy and Research Institute of Life Pharmaceutical Sciences, Sunchon National University, Suncheon-57922, Republic of Korea.

[3] Department of Pharmaceutical Chemistry, Jouf University, Sakaka, Al Jouf-2014, Saudi Arabia.

[4] School of Pure & Applied Physics, M.G. University, Kottayam, Kerala, India.

[5] Department of Pharmacology, Grace College of Pharmacy, Palakkad, India.

[6]Department of Pharmaceutical Chemistry, Nirmala college of Health Science, Chalakudy-680311, India

[7] Department of Pharmaceutical Chemistry, College of Pharmaceutical Sciences, Government Medical College Trivandrum, India

[#]Authors contributed equally.

[*]Corresponding Author: Bijo Mathew (B. Mathew) (bijovilaventgu@gmail.com)

Hoon Kim (H. Kim) (hoon@sunchon.ac.kr)

View Article Online
DOI: 10.1039/C8MD00399H

Abstract

A series of 13 phenyl substituted thiosemicarbazones (**SB1**-**SB13**) were synthesized and evaluated for their inhibitory potential towards human recombinant monoamine oxidase A and B (MAO-A and MAO-B, respectively) and acetylcholinesterase. The solid state structure of **SB4** was ascertained by single X-ray diffraction technique. Compounds **SB5** and **SB11** were potent for MAO-A (IC_{50} 1.82 ± 0.14) and MAO-B (IC_{50} 0.27 ± 0.015 μM), respectively. Furthermore, **SB11** showed high selectivity index (SI > 37.0) for MAO-B. The effects of fluorine orientation revealed that **SB11 (***m*-fluorine) showed 28.2 times higher inhibitory activity than **SB12 (***o*-fluorine) against MAO-B. Furthermore, inhibitions by **SB5** and **SB11** against MAO-A and MAO-B, respectively, were recovered to near reference levels in reversibility experiments. Both **SB5** and **SB11** showed competitive inhibition modes, with K_i values of 0.97 ± 0.042 and 0.12 ± 0.006 μM, respectively. These results indicate that **SB5** and **SB11** are selective, reversible and competitive inhibitors of MAO-A and MAO-B, respectively. Compounds **SB5**, **SB7** and **SB11** show moderate inhibition against acetylcholine sterase with IC_{50} values of 35.35 ± 0.47, 15.61 ± 0.057 and 26.61 ± 0.338 μM, respectively. Blood-brain barrier (BBB) permeation was studied using parallel artificial membrane permeation assay (PAMPA) method. Molecular docking studies were carried out by AutoDock4.2.

Keywords: Thiosemicarbazones, Monoamine oxidase, Acetylcholinesterase, Selective reversible inhibitor, Molecular docking, PAMPA-BBB.

View Article Online
DOI: 10.1039/C8MD00399H

Introduction

The role of monoamine oxidases (MAOs) in brain neurochemistry is mainly connected with the oxidative deamination of biogenic amines (BA) [1]. The regulation of amines such as adrenaline, nor-adrenaline, melatonin and serotonin are predominantly metabolized by MAO-A, whereas benzylamine and phenylethylamine are controlled by MAO-B. Both types of MAO isoforms have common substrates such as dopamine and tyramine [2, 3]. The selective types of MAO inhibitors (MAOIs) have a great impact in treating various psychiatric and neurodegenerative disorders by depleting MAO levels in the brain [4]. Serotonin concentration maintained by the inhibitors of MAO-A shows superior antidepressant activity [5]. Conversely, the end-products, hydrogen peroxide and reactive oxygen species (ROS), produced during dopamine metabolism by MAO-B, generate oxidative stress and apoptosis in dopamine producing cells. These highly reactive toxic radicals produce neural toxicity which may be the prime indications for Alzheimer's and Parkinson's diseases (AD & PD) [6]. Hence, selective MAO-B inhibitors are highly recommended as co-adjuvant therapy for treating AD and PD patients [7, 8].

The current scenario of PD therapy focuses on restoring the level of dopamine in the brain and thereby curtailing the motor symptoms [9]. This therapy is accelerated by the administration of dopamine precursors (L-dopa), dopamine agonists, catechol-*O*-methyltransferase (COMT) and MAO-B inhibitors such as selegiline and rasagiline (highly selective and irreversible) [10]. The molecules which have a closer acetylcholinesterase (AChE) and MAO-B affinities are able to limit the neurotoxicity related with sources of ROS in age related AD diseases [11]. In 2011, the molecule ladostigil, a dual inhibitor of both AChE and MAO-B designed by Youdim, entered into the phase II clinical trial for the treatment of AD [12]. Considering the complex pathogenetic factors of various

View Article Online
DOI: 10.1039/C8MD00399H

neurodegenerative diseases, it is highly appropriate to recommend selective MAO-B inhibitors with cocktail therapy to trigger the multi-targets associated with the diseases.

The MAO-B inhibitors currently in use are the irreversible type, having a covalent bond to the FAD unit of the inhibitor binding cavity (IBC) of the enzyme [13]. Disruption of target, poor ADME profile and increased duration of action occur due to this irreversible binding. Hence, the development of reversible MAO-B inhibitors has a greater therapeutic value in treating neurodegenerative diseases [14]. Some of the evidence also document that mild symptomatic benefits were gained by the administration of moclobemide (a reversible MAO-A inhibitor) when combined with levodopa for the treatment of PD [15, 16]. Recently, many small molecules like chalcones, coumarins and chromones have a considerable potential for the development of MAO-A/MAO-B inhibitors with a highly selective and reversible mode of inhibition [17-

From a chemical point of view, thiosemicarbazones are thiourea linked with an azomethine scaffold, and are the key intermediates for the synthesis of 2-amino-1,3,4-thiadiazoles via a ring chain tautomerism mechanism [20, 21]. Besides this, thiosemicarbazones are excellent chelators of transition metals such as zinc (Zn), copper (Cu) and iron (Fe), which are potent inhibitors of various carcinogenesis inducing pathways [22]. In the past, many efforts have addressed the development of thiosemicarbazones based MAOIs [23-29]. Moreover, the cyclized form of thiosemicarbazones from chalcones afforded N-thiocarbamoyl pyrazolines, which show a remarkable inhibition profile against MAOs [30-34]. The presence of hydrazine units in thiosemicarbazide also afforded a number of hydrazone scaffolds via the acid catalyzed nucleophilic addition mechanism [35]. Numerous studies recommend the multi-potent MAO and cholinesterase inhibitors for treating AD and PD [36, 37]. Accordingly, this work describes the synthesis of phenyl substituted

View Article Online
DOI: 10.1039/C8MD00399H

thiosemicarbazones, the MAO and acetylcholinesterase inhibition studies, and kinetics of the inhibition mechanism of MAOs using the Lineweaver-Burk plot, reversibility mode, and blood - brain barrier (BBB) permeation assays. Finally, the lead molecules from the *in vitro* results were subjected to molecular docking studies to elucidate the binding interactions of both MAO-A and B.

Result and discussion

Chemistry

The target aryl thiosemicarbazones were synthesized as presented in Scheme 1. Synthesis was accomplished by the single step reaction between commercially available thiosemicarbazide hydrochloride and various substituted benzaldehydes. In the ^{1}H-NMR spectra, a sharp singlet peak observed between 7.71-7.89 is ascribed to the azomethine (-CH=N-) proton. The down field of proton of the NH group attached to the thiocarbamoyl unit is observed in the range between 9.18-9.88. Two broad singlets were found at 6.23-7.25 and 7.23-7.26, corresponding to the terminal NH_2 group. ^{13}C NMR spectra displayed carbothioamide groups for **SB1**–**SB13** between δ180.60–184.30. All spectral characterizations are in full agreement with previous literatures [38-40]. The solid state structure of **SB4** was ascertained by the single X-ray diffraction technique, and the ORTEP diagram is depicted in Fig.1. Mass spectra of all fluorinated chalcones showed intensive molecular ions, assisting the structure of the targeted compounds.

View Article Online
DOI: 10.1039/C8MD00399H

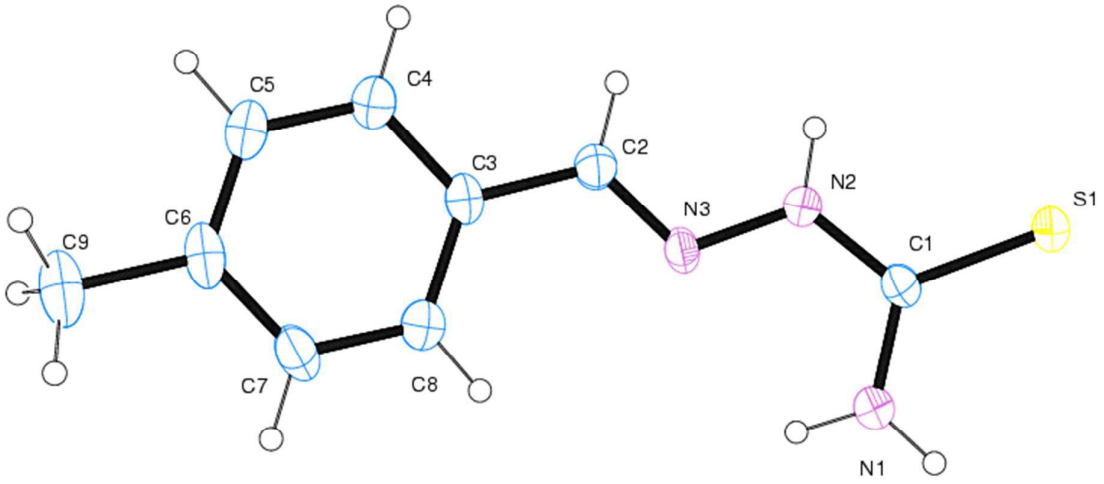

Fig. 1 ORTEP diagram of compound **SB4**

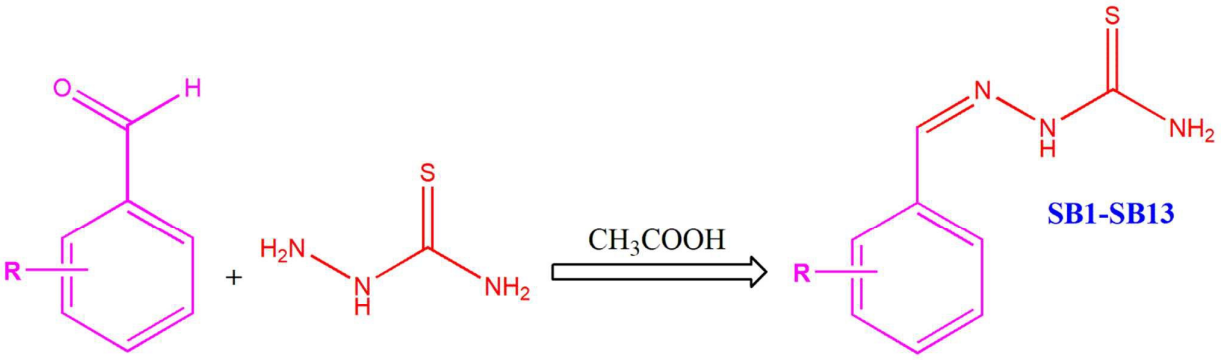

R		R	
SB1	:H	SB8	:4-Cl
SB2	:4-OH	SB9	:4-Br
SB3	:4-OCH_3	SB10	:4-F
SB4	:4-CH_3	SB11	:3-F
SB5	:4-$N(CH_3)_2$	SB12	:2-F
SB6	:4-C_2H_5	SB13	:4-CF_3
SB7	:4-NO_2		

Scheme 1 Synthetic route of aryl thiosemicarbazones

View Article Online
DOI: 10.1039/C8MD00399H

Monoamine oxidase inhibition studies

Inhibition profile of aryl substituted thiosemicarbazones. Six different compounds of the derivatives showed higher inhibitory activities (more than 50%) against MAO-A or MAO-B, while the other compounds were not effective (Table 1). Compounds **SB3**, **SB5**, and **SB6** showed efficient inhibition against MAO-A with IC_{50} values of 4.99 ± 0.25, 1.82 ± 0.14, and 5.98 ± 0.15 μM, respectively. Compounds **SB7**, **SB11**, and **SB12** were also effectively inhibitory against MAO-B with IC_{50} values of 1.43 ± 0.014, 0.27 ± 0.015, and 7.61 ± 0.49 μM, respectively. All 6 compounds showed good selectivity, and **SB5** and **SB11** were the most potent for MAO-A and MAO-B, respectively. Furthermore, **SB11** showed high selectivity index (SI > 37.0) for MAO-B with a low IC_{50} value (0.27 μM), suggesting it a good candidate for selective MAO-B inhibition. Considering the structural comparisons, we concluded that based on their IC_{50} values, the *m*-fluorine substitution of the compounds (**SB11**) showed 28.2 times higher inhibitory activity against MAO-B than *o*-fluorine substitution (**SB12**) and > 37.0 times potent than *p*-fluorine (**SB10**) (Table 1). However, the substituent *p*-NO_2 (**SB7**) was more effective than the *p*-fluorine substitution (**SB10**).

The potency of **SB5** for MAO-A (IC_{50} = 1.82 μM) was lower than **IM5** (IC_{50} = 0.30 μM), which is a synthesized imidazole bearing chalcone derivative of the eleven series and is the most potent for MAO-A reported by our group recently [41]. However, the SI value of **SB5** (0.18) in this study was > 4.2 times than **IM5** (0.75). The potency of **SB11** for MAO-B (IC_{50} = 0.27 μM) was higher than **IM4** (IC_{50} = 0.32 μM), which is another derivative and the most potent for MAO-B in the **IM** series. Similar to **SB5**, the SI value of **SB11** (> 37.0) was >11.2 times higher than the **IM4** (3.3). Although the potency of **SB11** for MAO-B was 6.4 times lower than that of the marketed drug lazabemide for MAO-B (IC_{50} = 0.042 μM), the relatively low molecular weight of **SB11** (MW = 197.2) is comparable to lazabemide (MW = 199.6) and smaller than **IM4** (MW = 288.3); it also has an IC_{50} value comparable to that of

View Article Online
DOI: 10.1039/C8MD00399H

lazabemide in the range of nanomolar concentration. The structural features of **SB11** were mainly divided as: (a) halogenated aryl system; (b) side chain with almost similar length; and (c) terminal amino group at the side chain. Similar type of features are seen in the potent MAO-B inhibitor (lazabemide) and are depicted in the Fig. 2. These structural features are responsible for the design and development of a new class of MAO-B inhibitors.

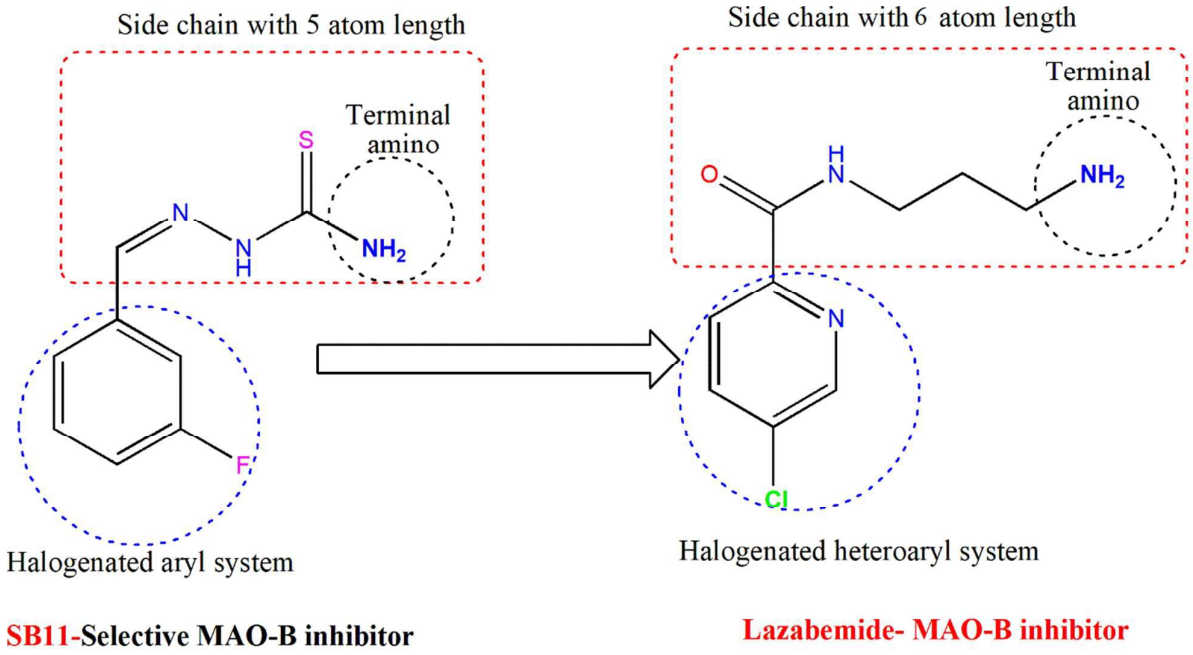

Fig. 2 Similarity based structure of **SB11** and standard MAO-B inhibitor

Structure activity relationship (SAR) analysis of MAO inhibition. Changes in the MAO inhibitory potency of the tested aryl thiosemicarbazones could be correlated to the effect of various electron donating and withdrawing groups anchored to the phenyl system. To explore the structure activity relationship of target compounds, we initially focused on variating substituents at *para* position of the phenyl system of aryl thiosemicarbazones. Unsubstituted aryl thiosemicarbazones are less effective against both MAO-A and MAO-B

View Article Online
DOI: 10.1039/C8MD00399H

with IC_{50} > 10.0 μM. Modifications in the position and orientation of substituent on the phenyl system result in a shift in this trend. The presence of electron donating groups (EDGs) such as methoxy, dimethylamino and ethyl on the *para* position of the phenyl system in compounds **SB3**, **SB5** and **SB6** significantly contribute to the activity ratio towards MAO-A. Furthermore, introduction of electron donating groups such as hydroxyl and methyl (**SB2** & **SB4**) results in a dramatic decrease in the activity. Hence, it is commonly recommended that EDGs with bulky groups on phenyl system of aryl thiosemicarbazones adapt well in the hydrophobic pocket of the inhibitor binding cavity (IBC) of MAO-A. Shifting of MAO-A selectivity was revealed after the introduction of an electron withdrawing nitro group. Presence of halogen such as chlorine, bromine and fluorine at the para position of aryl thiosemicarbazones had no impact on the MAO-B inhibition. In particular, shifting of fluorine atom to the *meta* position makes to be more potent MAO-B inhibition (**SB11**) with Ki value of 0.12 ± 0.006 μM. The inhibition constant was found to be better than the standard hMAO-B inhibitor (irreversible type) which is reported previously by our research group [42-50].

View Article Online
DOI: 10.1039/C8MD00399H

Table 1 Inhibition of recombinant human MAO enzymes and acetylcholinesterase by aryl substituted aryl thiosemicarbazones[a]

Compounds	Residual activity at 10 μM (%)		IC_{50} (μM)			SI[b]
	MAO-A	MAO-B	MAO-A	MAO-B	AChE	
SB1	83.5 ± 0.7	75.5 ± 0.7	> 10.0	> 10.0	> 40.0	
SB2	66.0 ± 1.4	87.5 ± 3.5	> 10.0	> 10.0	> 40.0	
SB3	37.5 ± 0.7	82.1 ±1.4	4.99 ± 0.25	> 10.0	36.14 ± 0.45	< 0.50
SB4	56.5 ± 0.7	91.5 ± 2.1	> 10.0	> 10.0	> 40.0	
SB5	16.5 ± 2.1	82.3 ± 1.4	1.82 ± 0.14	> 10.0	35.35 ± 0.47	< 0.18
SB6	36.0 ± 5.7	86.2 ± 1.4	5.98 ± 0.15	> 10.0	26.72 ± 0.006	< 0.60
SB7	75.5 ± 3.5	7.5 ± 0.7	> 10.0	1.43 ± 0.014	15.61 ± 0.057	> 6.99
SB8	76.0 ± 1.4	60.5 ± 2.1	> 10.0	> 10.0	> 40.0	
SB9	59.5 ± 0.7	82.5 ± 4.9	> 10.0	> 10.0	31.12 ± 0.44	
SB10	84.5 ± 3.5	86.5 ± 2.1	> 10.0	> 10.0	37.93 ± 0.57	
SB11	75.5 ± 2.1	3.0 ± 1.4	> 10.0	0.27 ± 0.015	26.61 ± 0.34	> 37.0
SB12	77.5 ± 0.7	33.5 ± 2.1	> 10.0	7.61 ± 0.49	30.84 ± 0.58	> 1.31
SB13	92.5 ± 0.7	77.5 ± 0.7	> 10.0	> 10.0	36.23 ± 0.44	
Toloxatone			0.92 ± 0.016	> 80		< 0.012
Lazabemide			> 80	0.042 ± 0.0010		> 1,900
Clorgyline			0.0071 ± 0.0003	1.69 ± 0.32		0.0042
Pargyline			1.31 ± 0.068	0.091 ± 0.005		14.4
Tacrine					0.23 ± 0.014	

[a]Results are expressed as means ± standard errors of duplicate experiments. Inhibitory activities for reference compounds of MAO and AChE were measured after preincubation with the enzymes for 30 min and 15 min, respectively.
[b]SI was expressed for MAO-B by dividing IC_{50} of MAO-A by that of MAO-B.

Kinetics. The inhibition modes of **SB5** and **SB11** for MAO-A and MAO-B, respectively, were analyzed by Lineweaver–Burk plots. The plots for **SB5** and **SB11** were linear and intersecting the *y*-axis (Fig. 3A & 3C). The K_i values determined by the secondary plot (slopes of Lineweaver–Burk plots vs. inhibitor concentrations) of MAO-A inhibition by **SB5** and MAO-B inhibition by **SB11** were 0.97 ± 0.042 and 0.12 ± 0.006 μM, respectively (Table

View Article Online
DOI: 10.1039/C8MD00399H

1, Fig. 3B & 3D). These results indicate that **SB5** and **SB11** are selective and reversible competitive inhibitors of MAO-A and MAO-B, respective

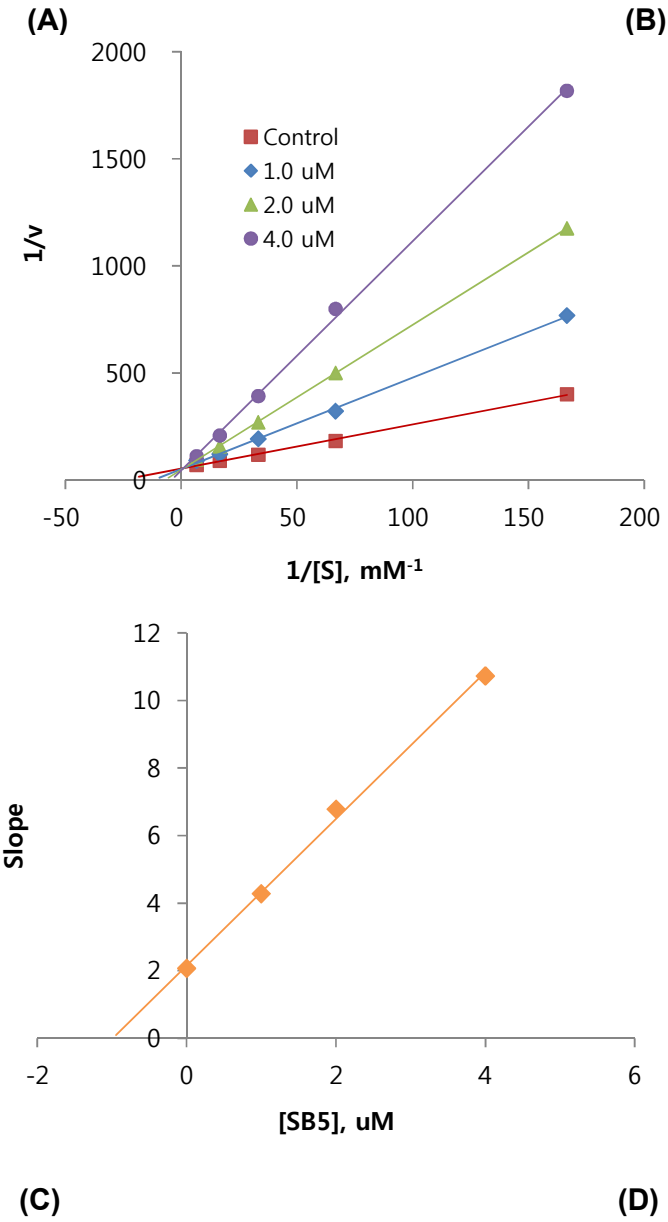

View Article Online
DOI: 10.1039/C8MD00399H

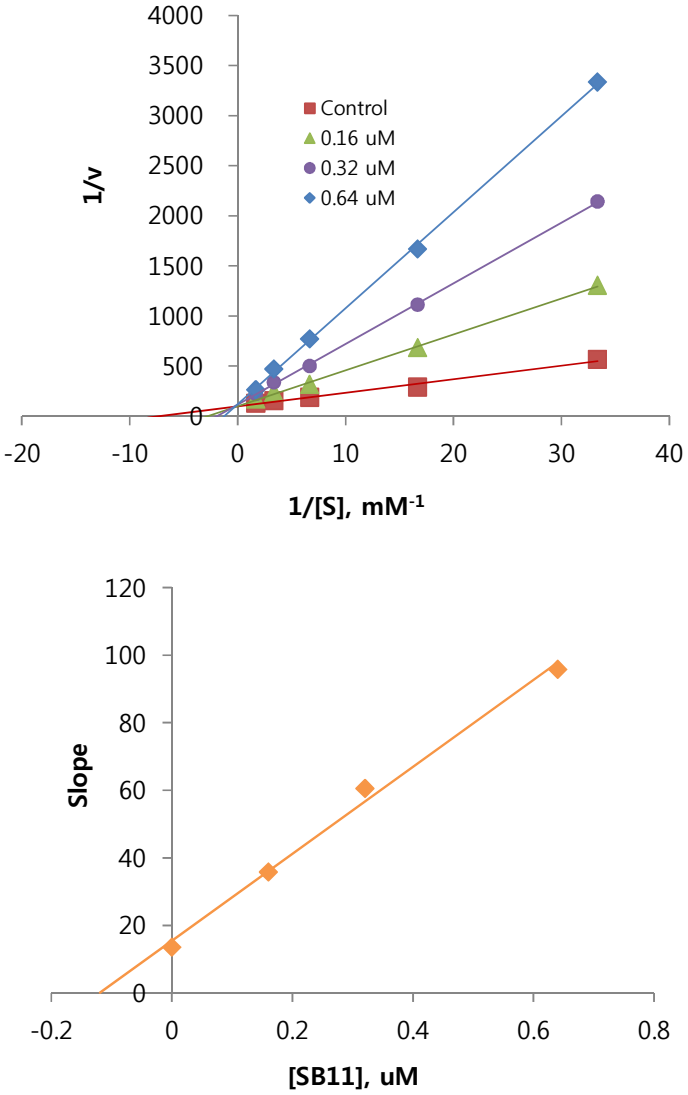

Fig. 3 Kinetic analyses of inhibitions of MAO-A by **SB5** (**A**) and MAO-B by **SB11** (**C**) using Lineweaver-Burk plots, and their respective secondary plots of slopes vs. inhibitor concentrations of **SB5** (**B**) and **SB11** (**D**).

Reversibility studies. No changes in the residual activities were observed when **SB5** and **SB11** were preincubated with MAO-A and MAO-B, respectively, for up to 30 min. In reversibility experiments, the A_U and A_D values obtained by **SB5** for MAO-A were 34.7% and 70.3%, respectively (Fig. 4A). Values for toloxatone (a reversible inhibitor) reference experiments for MAO-A were 30.7% and 74.0%, respectively, and the values for clorgyline

View Article Online
DOI: 10.1039/C8MD00399H

(an irreversible inhibitor) were 21.4% and 19.8%, respectively. The inhibition by toloxatone was greatly recovered by dialysis, while inhibition by clorgiline was not recovered. Similar to these results, the activity by **SB5** was recovered close to the reversible reference level. The enzymatic activity of the MAO-B by **SB11** revealed A_U and A_D values of 27.4% and 81.0%, respectively (Fig. 4B); values for lazabemide were 29.5% and 86.9%, respectively, and for pargyline were 27.9% and 32.0%, respectively. MAO-B inhibition by pargyline was not recovered by dialysis, whereas the activity by lazabemide was greatly recovered, similar to the recovery to near reference levels for inhibitory activity by **SB11**. These results indicate that analogues **SB5** and **SB11** are reversible inhibitors for MAO-A and MAO-B, respectively.

View Article Online
DOI: 10.1039/C8MD00399H

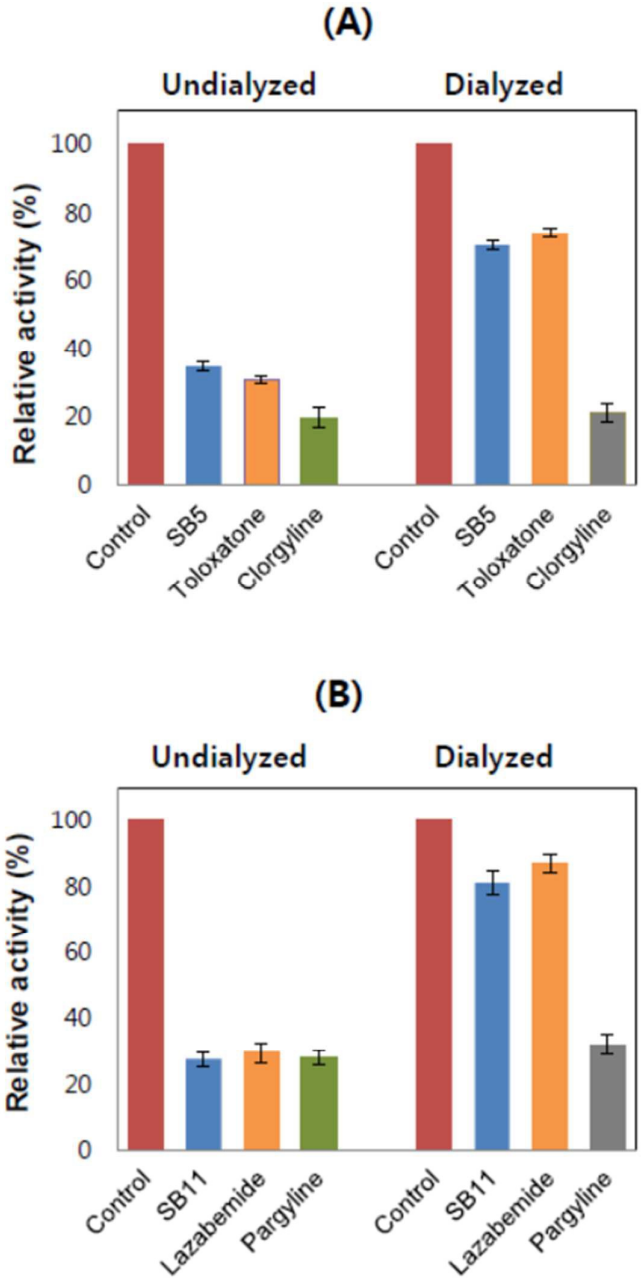

Fig. 4 Reversibility of MAO enzymes by aryl substituted thiosemicarbazones. MAO-A and MAO-B were inhibited at approximately 2 × IC_{50} by **SB5** (A) and **SB11** (B), respectively, and the activities were recovered by dialysis experiments against 100 mM sodium phosphate (pH 7.2) before measuring the residual activities. Concentrations of inhibitors and references used: **SB5**, 3.6 μM; toloxatone, 2.0 μM; clorgyline, 0.014 μM; **SB11**, 0.54 μM; lazabemide, 0.08 μM; pargyline, 0.20 μM.

View Article Online
DOI: 10.1039/C8MD00399H

Acetylcholinesterase inhibition

As presented in Table 1, it was noted that all the compounds are moderate and less potent than the reference compound tacrine for AChE inhibition. Considering the type of substitution at the phenyl ring, the inhibitory potency against AChE clearly favored the electron withdrawing nitro group at the *para* position of phenyl system (**SB7,** IC_{50} 15.61 ± 0.057 μM). According to the data, the presence of chlorine or hydroxyl group is not crucial for imparting the inhibitory potential against AChE in aryl thiosemicarbazones. Furthermore, fluorine orientation also showed moderate inhibition in titled compounds for AChE inhibition. The *ortho*- and *meta*-substituted analogue **SB12** and **SB11** show slightly higher AChE inhibitory activities compared to the *para*-substituted analogue S**B10,** likely being MAO-B inhibition.

Blood-brain barrier (BBB) permeation assay

An essential requirement for successful CNS drugs is the ability to cross the BBB, Which is determined using the parallel artificial membrane permeation assay (PAMPA). According to the limits established by Di et al., the BBB permeation test compounds are classified as follows: [51].

CNS+ (high BB permeation predicted): Pe ($\times 10^{-6}$ cms^{-1}) - > 4.00

CNS- (high BB permeation predicted): Pe ($\times 10^{-6}$ cms^{-1}) - > 2.00

Table 2 indicates the permeability of PAMPA-BBB assay of commercial drugs and the top ranked 6 aryl thiosemicarbazones. Our results indicate that all the tested thiosemicarbazones are capable of crossing the BBB to target the MAO-A and MAO-B enzymes in the central nervous system (CNS), which is consistent with our design strategy.

View Article Online
DOI: 10.1039/C8MD00399H

Table 2 PAMPA-BBB of aryl thiosemicarbazones and commercial drugs

Compounds[a]	Bibliography *Pe* ($\times 10^{-6}$ cms^{-1})[b]	Experimental *Pe* ($\times 10^{-6}$ cms^{-1})[c]	Prediction
SB3	-	11.24 ± 0.44	CNS+
SB5	-	10.14 ± 0.56	CNS+
SB6	-	09.44 ± 0.65	CNS+
SB7	-	12.78 ± 0.45	CNS+
SB11	-	13.12 ± 0.54	CNS+
SB12	-	10.33 ± 0.22	CNS+
Testosterone	17.0	17.33 ± 0.12	CNS+
Progesterone	9.3	08.13 ± 0.42	CNS+
Dopamine	0.2	0.21 ± 0.01	CNS-
Hydrocortisone	1.8	1.71 ± 0.02	CNS-

[a] Compounds were dissolved in DMSO to a concentration of 5 mg/mL and diluted with PBS/EtOH (70:30). The final concentration of compound was 100 µg/mL.

[b] Taken from [reference 51]

[c] Values are expressed as the mean ± SEM of three independent experiments.

Molecular docking

From the *in vitro* results, it is evident that compounds **SB5** and **SB11** show a good inhibitory profile towards MAO-A and MAO-B, respectively, in the micro molar range. We

View Article Online
DOI: 10.1039/C8MD00399H

therefore attempted to investigate the hypothetical binding modes of the respective compounds in the IBC of isoenzymes. Of the 50 runs in docking methodology, we selected the highest binding energy in the largest cluster for hypothetical binding pose. The binding mode of **SB5** (hMAO-A inhibitor) is shown in Fig. 5. The presence of imino nitrogen and terminal amino group in **SB5** contributes significant hydrogen bonding interactions with the TYR444 and the N5 atom of the flavin adenine dinucleotide (FAD) unit of MAO-A, respectively. **SB5** adopts an 'L' type configuration in which the aryl thiosemicarbazone unit is accommodated by the facing FAD unit with a hydrogen bond of distance 2.15 Å surrounded by the aromatic cage of TYR444 and TYR407. The position and close proximity towards the FAD unit of **SB5** may enhance its binding energy towards MAO-A.

The binding mode of potent MAO-B inhibitor **SB11** is shown in Fig. 6. The entrance cavity of the MAO-B leading to the substrate cavity is hydrophobic in nature [52]. ILE199 and TYR326 are the side chains responsible for the separation and fusion between the entrance and substrate cavity, depending on the nature of the bound inhibitor [53-56]. The *meta* substituted fluorine of the phenyl system of **SB11** is efficiently accommodated in the entrance cavity of the MAO-B. This lipophilic environment enhances the binding affinity of **SB11** towards the IBC of MAO-B. The terminal amino group of thiosemicarbazone shows a significant hydrogen bonding with GLN206 and the electron rich thiocarbamoyl group of **SB11** surrounded by the aromatic cage of TYR398 and TYR435 nearer to the FAD unit.

View Article Online
DOI: 10.1039/C8MD00399H

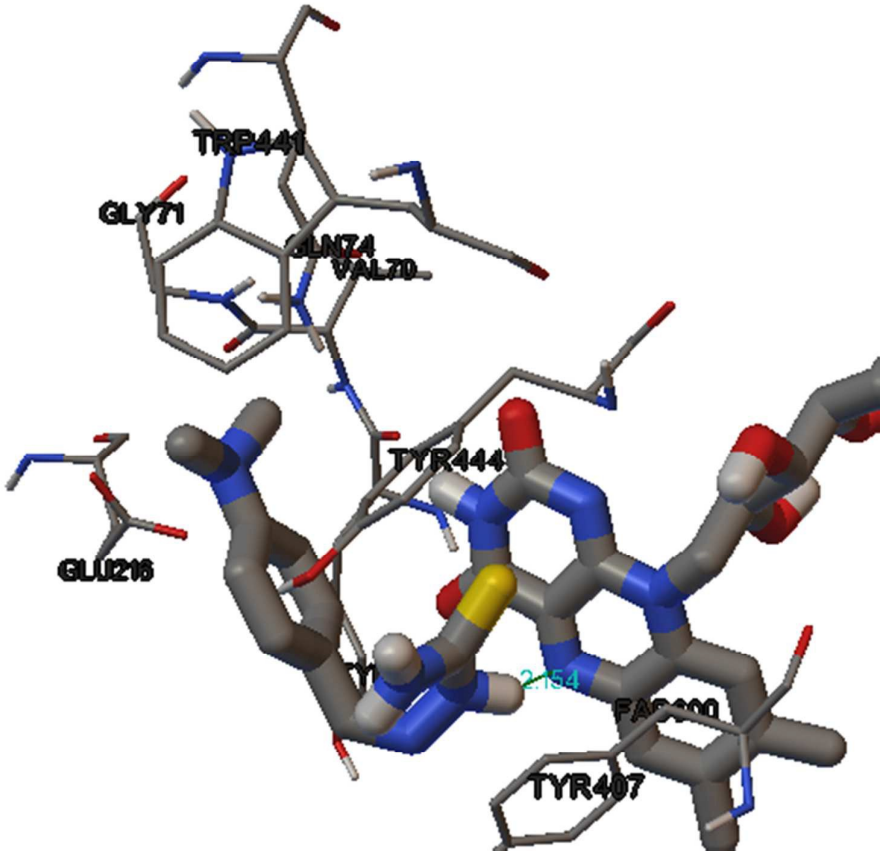

Fig. 5 SB5 in the active site of MAO-A

View Article Online
DOI: 10.1039/C8MD00399H

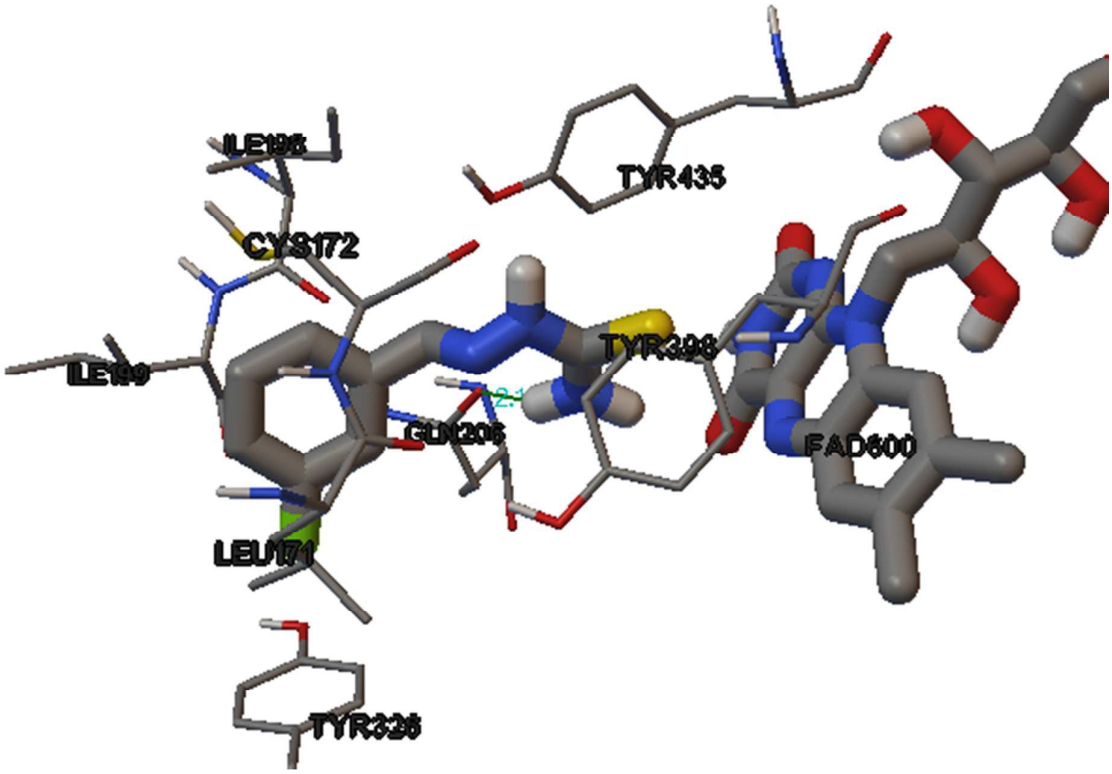

Fig. 6 **SB11** in the active site of MAO-B

Conclusions

To summarize our results, various aryl thiosemicarbazones with different electron donating and withdrawing environments were synthesized, characterized and evaluated for their MAO inhibitory and blood brain barrier permeation potential. The representative compounds **SB5** and **SB11** were potent for MAO-A and MAO-B, respectively, with reversible and competitive mode of inhibition, having IC_{50} values of 1.82 ± 0.14 and 0.27 ± 0.015 μM, respectively. The results explicate that nature and orientation of groups on the aryl system of titled scaffold can bestow significant selectivity profile on both MAO-A and MAO-B. The SAR revealed that presence of an electron donating bulky group produces good selectivity towards MAO, and at the same the time electron withdrawing nitro group in the same position shifts the selectivity

View Article Online
DOI: 10.1039/C8MD00399H

to MAO-B. The presence of halogen at the *para* position of the phenyl ring has no impact on MAO inhibition, but shifting of fluorine to the *meta* position dramatically results in good MAO-B inhibition with a high selectivity index. Compounds **SB5**, **SB7** and **SB11** show moderate inhibition against acetylcholinesterase with IC_{50} values of 35.35 ± 0.47, 15.61 ± 0.057 and 26.61 ± 0.338 μM, respectively. PAMPA studies revealed that the representative molecules are able to cross the blood-brain barrier, which is a pre-requisite of CNS drug design for the treatment of various neurodegenerative and psychiatric disorders. Molecular modelling studies identified that presence of the imino nitrogen and terminal amino group of **SB5** contributed significant hydrogen bonding interactions with the TYR444 and N5 atom of flavin adenine dinucleotide (FAD) unit of MAO-A, and *m*-fluorine of the phenyl system of **SB11** efficiently accommodated in the entrance cavity of the MAO-B. Also, the terminal amino group of thiosemicarbazone formed a significant hydrogen bonding with GLN206 of MAO-B.This study has thus provided new insights into the SARs of various aryl thiosemicarbazones compounds towards MAO inhibition and could possibly afford new attractive and more promising mutli-targeted ligands for the treatment of AD and PD.

Experimental

Chemistry

A mixture of thiosemicarbazide hydrochloride and substituted benzaldehyde in the presence of catalytic acetic acid was stirred for 3-4 hours. The resultant mixture was refluxed for 4-5 hours and poured onto crushed ice. The formed solid was washed with water until it was free from the acid, filtered and crystallized with ethanol. The following13 phenyl substituted thiosemicarbazones (**SB1**-**SB13**) were procured:

View Article Online
DOI: 10.1039/C8MD00399H

(2*E*)-2-benzylidenehydrazine-1-carbothioamide (**SB1**): Yellowish white; Yield: 76%; m.p: 126-128°C. ^{1}H NMR (400 MHz, $CDCl_3$)δ: 6.40 (s, 1H, NH_2), 7.23 (s, 1H, NH_2), 7.44-7.42 (m, 3H, J= 8Hz, Ar-H), 7.66-7.64 (d, 2H, J= 8Hz, Ar-H), 7.86 (s, 1H, -CH=N-), 9.60 (s, 1H, =N-NH-C=S). ^{13}C-NMR (100 MHz, $CDCl_3$) δ: 182.6 (C=S), 142.8 (CH=N), 134.3 (Ar-C1), 131.0 (Ar-C4), 129.3 (Ar-C2 & Ar-C6), 128.6 (Ar-C3 & Ar-C5). ESI-MS (*m/z*): Calculated- 179.24, Observed-361.23.

(2*E*)-2-[(4-hydroxyphenyl)methylidene]hydrazine-1-carbothioamide (**SB2**): Pale yellow; Yield: 63%; m.p: 210-212°C. ^{1}H NMR (400 MHz, $CDCl_3$)δ: 5.21 (s, IH, Ar-OH) 6.77, (s, 1H, NH_2), 6.94-6.92 (d, 2H, J= 8Hz, Ar-H), 7.28 (s, 1H, NH_2), 7.66-7.64 (d, 2H, J= 8Hz, Ar-H), 7.77 (s, 1H, -CH=N-), 9.56 (s, 1H, =N-NH-C=S). ^{13}C-NMR (100 MHz, $CDCl_3$) δ: 181.3 (C=S), 160.2 (Ar-C4), 142.37 (CH=N), 130.3 (Ar-C2 & Ar-C6), 125.2 (Ar-C1), 118.2 (Ar-C3 & Ar-C5). ESI-MS (*m/z*): Calculated- 195.24, Observed-195.23.

(2*E*)-2-[(4-methoxyphenyl)methylidene]hydrazine-1-carbothioamide (**SB3**): Yellowish; Yield: 78%; m.p: 150-152°C. ^{1}H NMR (400 MHz, $CDCl_3$)δ: 3.84 (s, 3H, OCH_3), 6.37 (s, 1H, NH_2), 6.92-6.90 (d, 2H, J= 8Hz, Ar-H), 7.26 (s, 1H, NH_2), 7.60-7.58 (d, 2H, J= 8Hz, Ar-H), 7.83 (s, 1H, -CH=N-), 9.66 (s, 1H, =N-NH-C=S). ^{13}C-NMR (100 MHz, $CDCl_3$) δ: 181.4 (C=S), 161.9 (Ar-C4), 145.2 (CH=N), 129.8 (Ar-C2 & Ar-C6), 128.9 (Ar-C1), 119.3 (Ar-C3 & Ar-C5), 55.4 (OCH_3). ESI-MS (*m/z*): Calculated- 209.26, Observed-209.25.

(2*E*)-2-[(4-methylphenyl)methylidene]hydrazine-1-carbothioamide (**SB4**): White; Yield: 82%; m.p: 155-157°C. ^{1}H NMR (400 MHz, $CDCl_3$)δ: 2.38 (s, 3H, CH_3), 6.46 (s, 1H, NH_2), 7.21-7.19 (d, 2H, J= 8Hz, Ar-H), 7.26 (s, 1H, NH_2), 7.54-7.52 (d, 2H, J= 8Hz, Ar-H), 7.88 (s, 1H, -CH=N-), 9.88 (s, 1H, =N-NH-C=S). ^{13}C-NMR (100 MHz, $CDCl_3$) δ: 181.6 (C=S), 145.3 (CH=N), 142.1 (Ar-C4), 132.2 (Ar-C1), 131.7 (Ar-C2 & Ar-C6), 131.4 (Ar-C3 & Ar-C5), 21.6 (CH_3). ESI-MS (*m/z*): Calculated- 193.26, Observed-193.25.

View Article Online
DOI: 10.1039/C8MD00399H

(2*E*)-2-{[4-(dimethylamino)phenyl]methylidene}hydrazine-1-carbothioamide (**SB5**): Yellowish; Yield: 81%; m.p: 190-192°C. ^{1}H NMR (400 MHz, $CDCl_3$)δ: 3.03 (s, 6H, $N(CH_3)_2$), 6.23 (s, 1H, NH_2), 6.68-6.66 (d, 2H, J= 12Hz, Ar-H), 7.26 (s, 1H, NH_2), 7.52-7.49 (d, 2H, J= 12Hz, Ar-H), 7.71 (s, 1H, -CH=N-), 9.18 (s, 1H, =N-NH-C=S). ^{13}C-NMR (100 MHz, $CDCl_3$) δ: 181.7 (C=S), 151.8 (Ar-C4), 141.4 (CH=N), 132.0 (Ar-C2 & Ar-C6), 123.5 (Ar-C1), 114.4 (Ar-C3 & Ar-C5), 41.9 ($N-(CH_3)_2$). ESI-MS (*m/z*): Calculated- 222.30, Observed-222.29.

(2*E*)-2-[(4-ethylphenyl)methylidene]hydrazine-1-carbothioamide (**SB6**): White; Yield: 84%; m.p: 125-126°C. ^{1}H NMR (400 MHz, $CDCl_3$)δ: 1.24-1.22 (t, 3H, J= 8Hz, CH_3), 2.70-2.68 (q, 2H, J= 8Hz, CH_2), 6.47 (s, 1H, NH_2), 7.24-7.22 (d, 2H, J= 8Hz, Ar-H), 7.26 (s, 1H, NH_2), 7.57-7.55 (d, 2H, J= 8Hz, Ar-H), 7.89 (s, 1H, -CH=N-), 9.92 (s, 1H, =N-NH-C=S). ^{13}C-NMR (100 MHz, $CDCl_3$) δ: 181.2 (C=S), 145.99 (CH=N), 137.3 (Ar-C4), 130.5 (Ar-C1), 129.8 (Ar-C2 & Ar-C6), 128.8 (Ar-C3 & Ar-C5), 33.5 (CH_2), 14.8 (CH_3). ESI-MS (*m/z*): Calculated- 207.29, Observed-207.00.

(2*E*)-2-[(4-nitrophenyl)methylidene]hydrazine-1-carbothioamide (**SB7**): Turmeric yellow; Yield: 82%; m.p: 220-222°C. ^{1}H NMR (400 MHz, $CDCl_3$)δ: 6.23 (s, 1H, NH_2), 6.68-6.66 (d, 2H, J= 8Hz, Ar-H), 7.26 (s, 1H, NH_2), 7.52-7.49 (d, 2H, J= 12Hz, Ar-H), 7.71 (s, 1H, -CH=N-), 9.20 (s, 1H, =N-NH-C=S). ^{13}C-NMR (100 MHz, $CDCl_3$) δ: 183.9 (C=S), 150.2 (Ar-C4), 143.4 (CH=N), 136.9 (Ar-C1), 131.3 (Ar-C2 & Ar-C6), 124.5 (Ar-C3 & Ar-C5). ESI-MS (*m/z*): Calculated- 224.23, Observed-224.22.

(2*E*)-2-[(4-chlorophenyl)methylidene]hydrazine-1-carbothioamide (**SB8**): Pale white; Yield: 83%; m.p: 175-177°C. ^{1}H NMR (400 MHz, $CDCl_3$)δ: 7.25 (s, 1H, NH_2), 7.40-7.38 (d, 2H, J= 8Hz, Ar-H), 7.26 (s, 1H, NH_2), 7.59-7.57 (d, 2H, J= 12Hz, Ar-H), 7.78 (s, 1H, -CH=N-), 9.33 (s, 1H, =N-NH-C=S). ^{13}C-NMR (100 MHz, $CDCl_3$) δ: 184.3 (C=S), 142.9

View Article Online
DOI: 10.1039/C8MD00399H

(CH=N), 137.3 (Ar-C4), 131.3 (Ar-C1), 130.6 (Ar-C2 & Ar-C6), 130.5 (Ar-C3 & Ar-C5). ESI-MS (*m/z*): Calculated- 213.68, Observed-213.67.

(2*E*)-2-[(4-bromophenyl)methylidene]hydrazine-1-carbothioamide (**SB9**): White; Yield: 85%; m.p: 140-142°C. ^{1}H NMR (400 MHz, $CDCl_3$) δ: 6.39 (s, 1H, NH_2), 7.26 (s, 1H, NH_2), 7.56-7.54 (d, 4H, J= 8Hz, Ar-H), 7.76 (s, 1H, -CH=N-), 9.29 (s, 1H, =N-NH-C=S). ^{13}C-NMR (100 MHz, $CDCl_3$) δ: 182.0 (C=S), 142.9 (CH=N), 131.2 (Ar-C1), 130.3 (Ar-C2 & Ar-C6), 130.2 (Ar-C3 & Ar-C5), 121.6 (Ar-C4).

ESI-MS (*m/z*): Calculated- 258.13, Observed-258.13.

(2*E*)-2-[(4-fluorophenyl)methylidene]hydrazine-1-carbothioamide (**SB10**): White; Yield: 82%; m.p: 120-122°C. ^{1}H NMR (400 MHz, $CDCl_3$)δ: 6.38 (s, 1H, NH_2), 7.40-7.38 (d, 2H, J= 8Hz, Ar-H), 7.26 (s, 1H, NH_2), 7.59-7.57 (d, 2H, J= 12Hz, Ar-H), 7.78 (s, 1H, -CH=N-), 9.33 (s, 1H, =N-NH-C=S). ^{13}C-NMR (100 MHz, $CDCl_3$) δ: 180.6 (C=S), 160.3 (Ar-C4), 142.2 (CH=N), 131.3 (Ar-C1), 130.6 (Ar-C2 & Ar-C6), 125.6 (d, $J_{C\text{-}F}$ = 62 Hz, Ar-C3 & Ar-C5). ESI-MS (*m/z*): Calculated- 197.23, Observed-197.23.

(2*E*)-2-[(3-fluorophenyl)methylidene]hydrazine-1-carbothioamide (**SB11**): Pinkish white; Yield: 79%; m.p: 155-157°C. ^{1}H NMR (400 MHz, $CDCl_3$)δ: 6.39 (s, 1H, NH_2), 7.26 (s, 1H, NH_2),7.56-7.54 (m, 4H, J= 8Hz, Ar-H), 7.76 (s, 1H, -CH=N-), 9.29 (s, 1H, =N-NH-C=S). ^{13}C-NMR (100 MHz, $CDCl_3$) δ: 182.2 (C=S), 166.2 (Ar-C3), 140.1 (CH=N), 136.6, (Ar-C5), 134.3 (Ar-C1), 125.3 (Ar-C6), 122.9 (d, $J_{C\text{-}F}$ = 64 Hz, Ar-C4), 121.6 (d, $J_{C\text{-}F}$ = 68 Hz, Ar-C2). ESI-MS (*m/z*): Calculated- 197.23, Observed-197.23.

(2*E*)-2-[(2-fluorophenyl)methylidene]hydrazine-1-carbothioamide (**SB12**): Yellowish grey; Yield: 82%; m.p: 121-123°C. ^{1}H NMR (400 MHz, $CDCl_3$)δ: ^{1}H NMR (400 MHz, $CDCl_3$)δ: 6.38 (s, 1H, NH_2), 7.12-7.10 (m, 2H, J= 8Hz, Ar-H), 7.26 (s, 1H, NH_2), 7.65-7.63 (m, 2H, J= 8Hz, Ar-H), 7.85 (s, 1H, -CH=N-), 9.66 (s, 1H, =N-NH-C=S). ^{13}C-NMR (100 MHz, $CDCl_3$) δ: 182.1 (C=S), 164.1 (Ar-C2), 143.6 (CH=N), 134.3, (d, $J_{C\text{-}F}$ = 68 Hz, Ar-C4),

View Article Online
DOI: 10.1039/C8MD00399H

130.2 (Ar-C6), 125.2 (Ar-C5), 122.6 (Ar-C1), 121.5 (Ar-C3). ESI-MS (*m/z*): Calculated-197.23, Observed-197.22.

(2*E*)-2-{[4-(trifluoromethyl)phenyl]methylidene}hydrazine-1-carbothioamide (**SB13**): Grey; Yield: 79%; m.p: 135-137°C. ^{1}H NMR (400 MHz, $CDCl_3$) δ: ^{1}H NMR (400 MHz, $CDCl_3$)δ: 6.44 (s, 1H, NH_2), 7.11-7.09 (d, 2H, J= 8Hz, Ar-H), 7.26 (s, 1H, NH_2), 7.37-7.35 (d, 2H, J= 12Hz, Ar-H), 7.87 (s, 1H, -CH=N-), 9.83 (s, 1H, =N-NH-C=S). ^{13}C-NMR (100 MHz, $CDCl_3$) δ: 181.4 (C=S), 160.3 (Ar-C4), 142.1 (CH=N), 138.4 (Ar-C1), 135.6 (Ar-C4), 129.2 (Ar-C2 & Ar-C6), 124.3 (q, $J_{C\text{-}F}$ = 278 Hz, Ar-C3 & Ar-C5), 123.6 (CF_3). ESI-MS (*m/z*): Calculated- 247.24, Observed-247.23.

Monoamine oxidase inhibition studies

Enzyme assays. Chemicals and enzymes were used as described previously. MAO activities were assayed by the continuous method using 0.06 mM kynuramine for MAO-A and 0.3 mM benzylamine for MAO-B as substrates, and reaction rates were expressed as absorbance changes per min. The K_m values of kynuramine and benzylamine obtained in this study were 0.040 mM and 0.15 mM, respectively, and the substrate concentrations used were 1.5 × and 2.0 × K_m values, respectively [57].

Analysis of inhibitory activities and enzyme kinetics. The inhibitions of MAO-A or MAO-B activities by the 13 compounds were primarily analyzed at a concentration of 10 μM. The IC_{50} values were then determined for 6 compounds showing more than 50% inhibitory activity, along with the reference compounds for reversible and irreversible inhibitors. Two potent compounds, **SB5** for MAO-A and **SB11** for MAO-B, were further investigated for time-dependent inhibition, kinetic studies for assessing the inhibition types, and K_i values of the compounds, as previously described [58].

Analysis of reversibility of the inhibitors. Reversibility experiments for the potent inhibitors were performed using the dialysis method, including reference compounds for

View Article Online
DOI: 10.1039/C8MD00399H

reversible and irreversible inhibitors, as previously described. The experiments were conducted at 3.6 μM **SB5** for MAO-A and 0.54 μM **SB11** for MAO-B in 100 mM sodium phosphate (pH 7.2) after preincubation for 30 min. Residual activities for undialyzed and dialyzed experiments were measured, and the relative activities for undialyzed (A_U) and dialyzed (A_D) experiments were calculated comparing with each control without inhibitor. The reversibility pattern was determined by comparing the relative A_U and A_D values [59].

Acetylcholinesterase inhibition

AChE inhibitory activity was assayed using the method developed by Ellman et al., with slight modifications. The reaction was assayed for 10 min at 412 nm using 0.2 U/ml of AChE (*Electrophorus electricus*, Type VI-S, Sigma) in 0.5 ml reaction mixture of 50 mM sodium phosphate (pH 7.5), in the presence of 0.5 mM 5,5'-dithiobis(2-nitrobenzoic acid) (DTNB) and 0.5 mM acetylthiocholine iodide (ACTI). For measurement of inhibitory activity, each inhibitor (and tacrine as a reference) was preincubated for 15 min with the enzyme prior to addition of DTNB and ACTI [60].

Blood-brain barrier (BBB) assay

The top ranked 6 synthesized thiosemicarbazones and the known commercial drugs were dissolved in DMSO at a final concentration of 5 mg/mL, followed by appropriate dilution with a mixture 70:30 of phosphate buffered saline solution and ethanol (PBS/EtOH) to give a final concentration of 25 μg/mL. The filter membrane in the donor microplate was coated with polar brain lipid (PBL) dissolved in docodecane (4 μg/mL, 20 mg/mL). A total of 200 μL of diluted solution and 300 μL of PBS/EtOH (70:30) were added to the donor and the acceptor wells, respectively. The donor filter plate was carefully placed on the acceptor plate, And the sandwich system was kept at 25°C for 16 h. The donor plate was carefully removed,

View Article Online
DOI: 10.1039/C8MD00399H

and the concentrations of the compounds and the commercial drugs in the acceptor, donor and the reference wells were measured with a UV plate reader [51].

Molecular docking

AUTODOCK4.2 software was employed for molecular docking studies for the lead molecules [61]. Preparation Wizard of Maestro-8.4 (Schrodinger LLC) was used to prepare the protein. Crystallographic models 2BXR (hMAO-A) and 2BYB (hMAO-B) were downloaded from www.rcsb.org [62]. Ligands were prepared through PRODRG webserver (http://davapc1.bioch.dundee.ac.uk/cgi-bin/prodrg) [63]. Grid preparation and the docking parameters are prepared on the basis of a reported method [64].

Conflict of Interest

There are no conflicts of interest to declare.

Acknowledgements

This research was supported by the Basic Science Research Program through the National Research Foundation (NRF) of Korea, which is funded by the Ministry of Education (2017R1D1A3B03028559) (To H. Kim).

References

[1] K.F. Tripton, Cell. Biochem. Funct. 4 (1986) 79-87.

[2] R.R. Ramsay, Curr. Pharm. Des. 19 (2013) 2529-2539.

[3] B. Kumar, Sheetal, A.K. Mantha, V. Kumar, RSC Adv. 6 (2016) 42660-42683.

[4] S. Carradori, D. Secci, A. Bolasco, P. Chiment, M. D' Asceenzio, Expert Opin. Ther. Pat. 22 (2012) 909-939.

View Article Online
DOI: 10.1039/C8MD00399H

[5] B. Mathew, J. Suresh, G.E. Mathew, S.A. Rasheed, J.K. Vilapurathu, P. Jayaraj, Curr. Enzyme Inhib. 11 (2015) 108–115.

[6] M.B. Youdim, Y.S. Bakhle, Br. J. Pharmacol. 147 (2006) S287-S296.

[7] M.B. Youdim, D. Edmondson, K.F. Tripton, Nat. Rev. Neurosci. 7 (2006) 295-309.

[8] P. Riederer, T. Muller. Expert Opin. Drug Metab. Toxicol.13 (2017) 233-240.

[9] B. Kumar, Sheetal, A.K. Mantha, B. Kumar, RSC Adv. 6 (2016) 42660–42683.

[10] C. Binda, E.M. Milczek, D. Bonivento, J. Wang, A. Mattevi, D.E. Edmondson, Curr. Top. Med. Chem. 11 (2011) 2788–2796.

[11] L. Pisani, M. Catto, F. Leonetti, O. Nicolotti, A. Stefanachi, F. Campagna, A. Carotti, Curr. Med. Chem. 18 (2011) 4568-4587.

[12] M. B. H. Youdim, M. B. H. Curr. Alzheimer Res. 3 (2006) 541-550.

[13] S. Carradori, R. Silvestri, J. Med. Chem. 85 (2015) 6717–6732.

[14] C. Binda, M. Li, F. Hubaìlek, N. Restelli, D.E. Edmondson, A. Mattevi, Proc. Natl. Acad. Sci. U.S.A. 100 (2003) 9750–9755.

[15] M.B. Youdim, M. Weinstock, Neurotoxicology 25 (2004) 243-250.

[16] K. Sieradzan, S. Channon, C. Ramponi, G.M. Stern, A.J. Lees, M.B. Youdim, J. Clin. Psychopharmacol. 15 (1995) 51S-59S.

[17] B. Mathew, A. Haridas, J. Suresh, G.E. Mathew, G. Ucar, V. Jayaprakash, Cent. Nerv. Syst. Agents Med. Chem. 16 (2016) 120–136.

[18] M.J. Matos, D. Vina, S. Vazque-Rodrigues, E. Uriarte, L. Santana, Curr. Top. Med. Chem. 12 (2012) 2210-2239.

[19] B. Mathew, G.E. Mathew, J.P. Petzer, A. Petzer, Comb. Chem. High. Throughput Screen. 20 (2017) 522-532.

[20] S. Kasayuki Uda. J. Heterocycl. Chem. 16 (1979) 1273-1278.

[21] K.N. Zelenin, O.R. Kuzenetsova, V.V. Alekseyev, P.B. Terentyev, V.V. Ovacharenko,

View Article Online
DOI: 10.1039/C8MD00399H

Tetrahedron 49(1993) 1257-1270.

[22] Y. Yu, D.S. Kalinowski, Z. Kovacevic, A.R. Siafakas, P.J. Jansson, C. Stefani, et al. J. Med. Chem. 52 (2009) 5271-5294.

[23] S. Tripathi, B.R. Pandaey, J.P. Barthwal, K. Kishor, K.P. Bhargava, Res. Commun. Chem. Pathol. Pharmacol. 22 (1978) 291-300.

[24] D.K. Agarwal, B.R. Pandaey, Res. Commun. Chem. Pathol. Pharmacol. 26 (1979) 525-531.

[25] F. Chimenti, E. Maccioni, D. Secci, A. Bolasco, A. Chimenti, A. Granese, et al., J. Med. Chem. 51 (2008) 4874-4880.

[26] R.K.P Tripathi, O. Goshain, S.R. Ayyannan, ChemMedChem 8 (2013) 462-474.

[27] R.K.P Tripathi, G.K. Rai, S.R. Ayyannan, ChemMedChem 11 (2016) 1145-1160.

[28] R.K.P Tripathi, M. Sasi, S.K. Gupta, S. Krishnamurthy, S.R. Ayyannan, J. Enzyme Inhib. Med. Chem. 33(2018) 37-57.

[29] R. Pignatello, S. Mazzone, F. Castelli, P. Mazzone, G. Raciti, G. Mazzone. Pharmazie 49 (1994) 272-276.

[30] N. Gokhan, A. Yesilada, G. Ucar, K. Erol, A.A. Bilgin, Arch.Pharm. (Weinheim) 336 (2003) 362-371.

[31] G. Ucar, N. Gokhan, A. Yesilada, A.A. Bilgin, Neurosci. Lett. 382 (2005) 327-331.

[32] S. Yabanoglu, G. Ucar, S. Gokhan, U. Salgin, A. Yesilada, A.A. Bilgin, J. Neural Trans (Vienna) 114 (2007) 769-773.

[33] D. Secci, S. Carradori, A. Bolasco, B. Bizzarri, M. D'Ascenzio, E. Maccioni, Curr. Top. Med. Chem. 12 (2012) 2240-2257.

[34] B. Mathew, J. Suresh, S. Anbazhagan, G.E. Mathew, Cent. Nerv. Syst. Agents Med. Chem. 13 (2013) 195-206.

[35] B. Mathew, J. Suresh, M.J. Ahasan, G.E. Mathew, D. Usman, P.N. Subramanyan, et al.,

View Article Online
DOI: 10.1039/C8MD00399H

Infect. Disord. Drug Targets 15 (2015) 76-88.

[36] D. Vina, M.J. Matos, M. Yanez, L. Santana, Uriarte, E. Med. Chem. Commun. 3 (2012) 213-218.

[37] W.J. Geldenhuys, K.S. Ko, H. Stinneft, C.J. Van der Schyf, Med. Chem. Commun. 2 (2011) 1099-1103.

[38] N. A. Soares, M.A. Almeida, C. Marins-Goulart, O.A, Chaves, A. Echevarria, M.C.C.de Oliveria. Bioorg. Med. Chem. Lett. 27 (2017) 3546-3550.

[39] G.R. Subhashree, J, Haribabu, S. Saranya, P. Yuvaraj, D. Krishnan, R. Karvenbu et al., J. Mol. Struct. 1145 (2017) 160-169.

[40] P. Liciano, C.B. Moraes, L.M. Alcantara, C.H. Franco, B. Pascoalino, L.H. Freitas-Junior et al., Eur. J. Med. Chem. 146 (2018) 423-434

[41] R. Sasidharan, S.C. Baek, S.L. Manju, H. Kim, B. Mathew, Biomed. Pharmacother. 106 (2018) 8-13.

[42] B. Mathew, G. Ucar, S.Y. Ciftci, I. Baysal, J. Suresh, G.E. Mathew, J. K.Vilapurathu, N.A. Moosa, N. Pullarottil, L. Viswam, A. Haridas, F. Fathima, Lett.Org. Chem. 12 (2015) 605–613.

[43] B. Mathew, G.E. Mathew, G. Ucar, I. Baysal, J. Suresh, J.K. Vilapurathu, A. Prakasan, J.K. Suresh, A. Thomas, Bioorg. Chem. 62 (2015) 22–29.

[44] B. Mathew, G.E. Mathew, G. Ucar, I. Baysal, J. Suresh, S. Mathew, A. Haridas, V. Jayaprakash, Chem. Biodivers. 13 (2016) 1046–1052.

[45] B. Mathew, G. Ucar, G.E. Mathew, S. Mathew, P.K. Purapurath, F. Moolayil, S. Mohan, S.V. Gupta, ChemMedChem 11 (2016) 2649–2655.

[46] B. Mathew, A. Haridas, G. Ucar, I. Baysal, A.A. Adeniyi, M.E.S. Soliman, M. Joy, G.E. Mathew, B. Lakshmanan, V. Jayaprakash, Int. J. Biol. Macromol. 91 (2016) 680–695.

View Article Online
DOI: 10.1039/C8MD00399H

[47] B. Mathew, A. Haridas, G. Ucar, I. Baysal, M. Joy, G.E. Mathew, B. Lakshmanan, V. Jayaprakash, ChemMedChem 11 (2016) 1161–1171.

[48] R. Sasidharan, S.L. Manju, G. Ucar, I. Baysal, B. Mathew, Arch. Pharm. 349 (2016) 627–637.

[49] B. Mathew, G.E. Mathew, G. Ucar, G.E. Mathew, E.K. Nafna, K.L. Lohidakshan, J. Suresh, Int. J. Biol. Macromol. 104 (2017) 1321–1329.

[50] B. Mathew, G. Ucar, C. Raphael, G.E. Mathew, M. Joy, K.E. Machaba, M.E.S. Soli man, ChemistrySelect 2 (2017) 11113-11119.

[51] L. Di, E.H. Kerns, K. Fan, O.J. McConnell, G.T. Carter. Eur. J. Med. Chem. 38 (200 3) 223-232.

[52] B. Mathew, A.A. Adeniyi, S. Dev, M. Joy, G. Ucar, G.E. Mathew, A.S. Pillay, M.E.S. Soliman, J. Phys. Chem. B 121 (2017) 1186–1203

[53] L. Novaroli, A. Daina, E. Favre, J. Bravo, A. Carotti, F. Leonetti, et al. J. Med. Chem. 49 (2006) 6264-6272.

[54] L. Legoabe, J. Kruger, A. Petzer, J.J. Bergh, J.P. Petzer, Eur. J. Med. Chem. 46 (2011) 5162-5174.

[55] S.J. Lan, L.F. Pan, S.S. Xie, X.B. Wang, L.Y. Kong, Med. Chem. Commun. 6 (2015) 592-600.

[56] S.J. Lan, T. Zang, Y.Liu, Y.Zahng, J.W. Hou, S.S. Xie et al., Med. Chem. Commun. 8 (2017) 471-478.

[57] S.C. Baek, H.W. Lee, H.W. Ryu, M.G. Kang, D. Park, S.H. Kim, Bioorg. Med. Chem. Lett. 28 (2018) 584-588.

[58] J. Suresh, S.C. Baek, S.P. Ramakrishnan, H. Kim, B. Mathew, Int. J. Biol. Macromol. 108 (2018) 660–664.

[59] H.W. Lee, H. Choi, S.J. Nam, W. Fenical, H. Kim, J. Microbiol. Biotechnol. 27 (2017)

View Article Online
DOI: 10.1039/C8MD00399H

785–790.

[60] G.L. Ellman, K.D. Courtney, V. Jr. Andres, R.M. Feather-Stone, Biochem Pharmacol. 7 (1961) 88-95.

[61] G.M. Morris, R. Huey, W. Lindstrom, M.F. Sanner, R.K. Belew, D.S. Goodsell, A.J. Olson, J. Comput. Chem. 30 (2009) 2785–2791.

[62] L. De Colibus, M. Li, C. Binda, A. Lustig, D.E. Edmondson, A. Mattevi, Proc. Natl. Acad. Sci. USA 102 (36) (2005) 12684–12689.

[63] A.W. Schuttelkopf, D.M. van Aalten, Acta Crystallogr. D Biol. Crystallogr. 60 (2004) 1355–1363.

[64] B. Mathew, J. Suresh, S. Anbazhagan, S. Dev, Biomed. Aging Pathol. 4 (2014) 297–301.

View Article Online
DOI: 10.1039/C8MD00399H

Graphical abstract

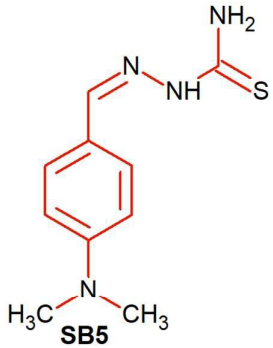

SB5

hMAO-A = 1.82 μM
hMAO-B = > 10 μM
AChE = 35.35 μM

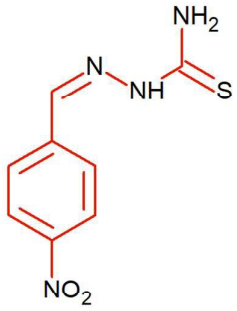

SB7

hMAO-A = > 10 μM
hMAO-B = 1.43 μM
AChE = 15.61 μM

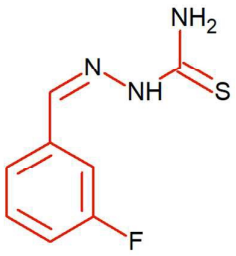

SB11

hMAO-A = > 10 μM
hMAO-B = 0.27 μM
AChE = 26.61 μM